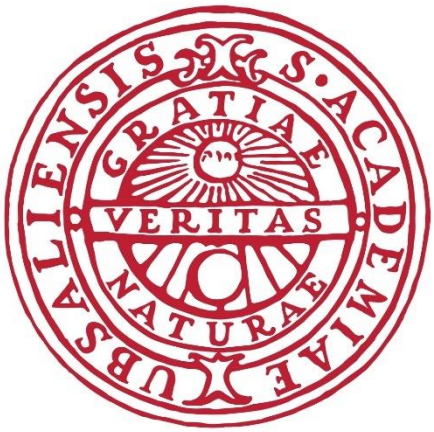

UPPSALA UNIVERSITET

5 Credits Project work in Physics & Astronomy (2017)

Ionospheric model of comet 67P including the effect of solar EUV attenuation

Kilian Hikaru Scheutwinkel

Supervised by Erik Vigren at the Swedish Institute of Space Physics

ABSTRACT

Comets are the most active around their perigees. The increased outgassing can lead to a coma thick enough to effectively absorb the solar EUV radiation, which engenders a self-shielding comet nucleus and inner layers of the ionosphere. This effect of self-shielding can be calculated by the attenuation of the sunlight according to the Beer-Lambert law. Here we focus on the perihelion of comet 67P/Churyumov-Gerasimenko, the target comet of the ESA Rosetta mission. We calculate attenuated photoionization frequencies and implement these into an ionospheric model constructed in a recent project work (by the same author). The ionization frequencies and ion number densities are calculated as a function of cometocentric distance and compared with the latest published peer-reviewed article by Heritier et al. (2017). Overall, the agreement is fairly good. The most significant difference is the discrepancy of number densities of O_2 ions, which is higher in our model by nearly an order of magnitude. This discrepancy is attributed to the fact that Heritier et al (2017) only considered charge transfer processes for the formation of O_2^+, while we identify photoionization of O_2 as the main production mechanism.

1. INTRODUCTION

67P/Churyumov-Gerasimenko is a Jupiter family comet and the target comet of the ESA *Rosetta* mission which resided and conducted measurements close to the comet for more than two years between the summer of 2014 and the end of September 2016. One of the outstanding results from the mission was the discovery of abundant molecular oxygen in the cometary coma (Bieler et al., 2015). *In situ* measurements by the Rosetta Orbiter Spectrometer for Ion and Neutral Analysis (ROSINA)/Double Focusing Mass Spectrometer (DFMS) revealed a ~4% mixing ratio of O_2 and a strong correlation with the water outgassing. This discovery lead to a re-investigation of data from the Giotto Mission to comet 1P/Halley. Indeed, the data was compatible with molecular oxygen at the level of ~4% in the coma, with respect to the most dominant species, H_2O (Rubin et al., 2015). As the formation sites and dynamical histories of the comets differ, these results suggest that high abundances of molecular oxygen may be a general feature of comets, which indicates an origin in the molecular cloud that predated our solar system.

In a previous project work by Scheutwinkel, 2017 (S17), we used the base model of Vigren & Galand (2013) and modified it to investigate how a high relative abundance of molecular oxygen (~5%) influence the ion composition throughout the ionosphere. We also investigated the ionospheric composition at different heliocentric distances hence changing the activity level of the nucleus and the ionization frequencies. Comparisons were made with the state-of-the-art ionospheric modeling by Heritier et al. (2017). S17 predicted a nearly an order of magnitude higher O_2^+ abundance than Heritier et al. (2017) with roughly the same conditions. S17 concluded that this discrepancy can be explained by photoionization of O_2^+, which was not included in the model of Heritier et al. (2017). Also, small discrepancies of other ion number densities near the surface could potentially be explained by the fact that S17 did assume constant ionization frequencies throughout the coma, whereas Heritier et al. (2017) took into account the attenuation of the solar EUV photons.

In the present work, we improve the work of S17 by numerically solving the Beer-Lambert equation as to include the above-mentioned attenuation effect. We also rescale some input parameters of the model to better match those of Heritier et al. (2017), allowing more relevant comparisons with their results. While the base of our model (numerical solution of coupled continuity equations accounting for outward radial transport) is described in S17 the updates are described in Section 2 (the full code is given in the Appendix). Results (including comparisons with Heritier et al., 2017) are presented and discussed in Section 3 while a summary with concluding remarks is given in Section 4.

2. MODEL DESCRIPTION

The base model of S17 has been used and further improved by including the attenuation effect of the solar EUV spectra. The attenuation of photons can be modeled by the Beer-Lambert law, which describes the exponential intensity loss due to an absorbing medium with an optical depth τ:

$$I(\lambda, z_0) = I_0(\lambda) \cdot \exp(-\tau(\lambda, z_0)) \quad (1)$$

The optical depth of a medium consisting of multiple neutral species j at altitude $z_0$with a vertical sun depends on the column density and wavelength dependent photoabsorption cross-sections:

$$\tau(\lambda, z_0) = \sum_j \sigma_{j,abs}(\lambda) \cdot \int_{z_0}^{\infty} n_j(z) \cdot dz \quad (2)$$

Now, the position of the Rosetta spacecraft with respect to the sun and the nucleus is playing an important role for the total solar irradiance. This can be solved geometrically and will modify equation (2). We introduce the solar zenith angle χ_0 for a spherically symmetric neutral number density distribution. For $\chi_0 \leq 90°$ the optical depth is modified according to (e.g., Rees, 1989):

$$\tau(\lambda, z_0) = \sum_j \sigma_{j,abs}(\lambda) \cdot \int_{z=z_0}^{\infty} n_j(z) \left[1 - \left(\frac{z_0}{z}\right)^2 \sin^2\chi_0\right] \cdot dz \quad (3)$$

where *z* is the cometocentric distance. For a given cometocentric distance the attenuation effect is more pronounced the higher the solar zenith angle is. As Rosetta typically resided near the terminator we use $\chi_0 = 89°$ throughout this work.

However, the integral of (3) cannot be easily solved analytically and a numerical approach to solve for the optical depth is used. The integral is calculated up to a cometocentric distance of 200 km with 0.1 km shells and evaluated for all altitudes z_0. The corresponding photoionization cross-sections of H_2O were taken from Schunk & Nagy (2009) and interpolated linearly into 1 nm wavelength bins. To compute the attenuated photoionization frequencies the Solar EUV spectra from Thermosphere Ionosphere Mesosphere Energy and Dynamics/ Solar EUV Experiment (TIMED/SEE) of 2015 March 1st was used. To get the frequencies from neutral *j* to ion *k* at a given altitude z_0 one use the following equation:

$$f_{j\to k}(z_0) = \int \sigma_{j\to k}(\lambda) \cdot I(\lambda, z_0)\, d\lambda \quad (4)$$

where $\sigma_{j\to k}$ is the partial photoionization cross-section of *j* yielding *k*. The "attenuated frequencies" are implemented in the existing source code (see S17 and Appendix) in order to calculate number densities of the ion species. The ionization frequencies for O_2 are assumed to be in constant ratio to the H_2O frequencies. The constant value is determined by the ratio of the unattenuated frequencies of O_2 to H_2O of S17.

3. RESULTS AND DISCUSSION

3.1 Attenuated frequency profiles

By using the perihelion settings of S17 (heliocentric distance *d*=1.25 AU) and an O_2:H_2O ratio of 1:99 we obtain H_2O partial photoionization frequencies according to Fig. 1. Note that while the observed relative abundance of O_2 was around 4% early on in the mission (as mentioned in Section 1) it was closer to 1% near perihelion (see e.g., Gasc et al., 2017); this lower mixing ratio was also considered by Heritier et al. (2017). Figure 1 shows an exponentially decreasing trend of about one order of magnitude the closer the photons reach the surface of the comet. This is due to the increasing density near the surface of the comet. According to our model, the attenuation effect is gathering a dominant role around a cometocentric distance of 20 – 50 km. Comparing Figure 1 with Fig. 4 of Heritier et al. (2017) one notices a discrepancy in magnitude; their values being smaller by more than 30%. This is caused by differences in the input parameters, in particular, different density profiles and consideration of different solar EUV spectra. By scaling the production rate to obtain values similar to Heritier et al. (2017) e.g. setting the neutral number density of $2 \cdot 10^6$ cm^{-3} at 400 km and by scaling the frequencies to match their unattenuated total H_2O photoionization frequency of $3.13 \cdot 10^{-7}$ s^{-1} we obtain frequencies according to Fig. 2. These are in good agreement with frequencies in Fig. 4 of Heritier et al. (2017).

There is still some discrepancy close to the nucleus with our values being slightly higher. This is caused by the fact that we consider a constant outgassing velocity while in the model of Heritier et al. (2017) the outward velocity is increasing with higher cometocentric distance (converging towards a constant value). Given matching neutral densities and velocities at 400 km, that is matching fluxes, and the fact that the velocities in the model of Heritier et al. (2017) are lower towards the surface implies that their neutral densities are higher towards the surface. As such the attenuation becomes more pronounced in their model.

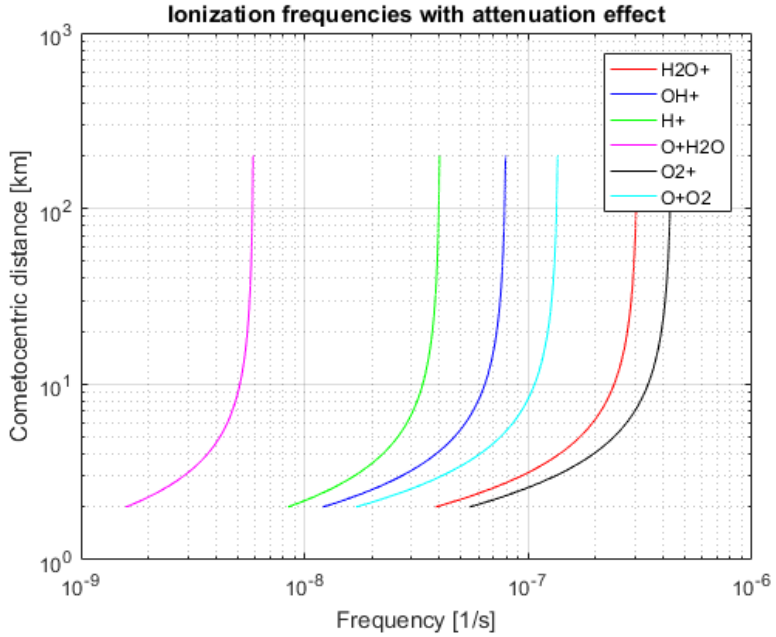

Figure 1: Partial photoionization frequencies of H_2O throughout the coma.

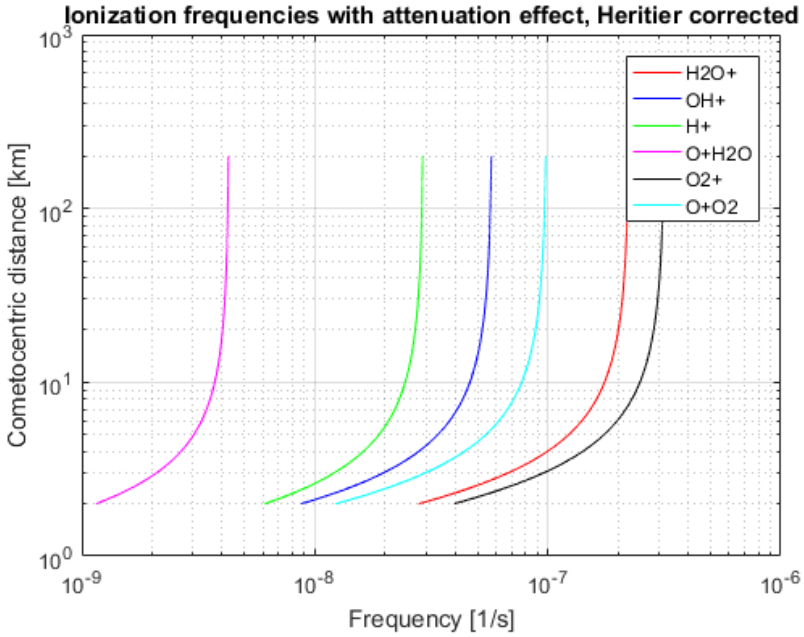

Figure 2: Partial photoionization frequencies of H_2O throughout the coma with background/irradiation conditions better matching the input of Heritier et al. (2017)

3.2. Ion number density profiles

For the ion number densities, we simulate three cases. Figure 3 represents the settings of S17 while Figure 4 is the simulation adjusted to the settings of Heritier et al. 2017 (neutral density of $2 \cdot 10^7$ cm^{-3} at 180 km, see their Fig. 7). In both cases an O_2:H_2O ratio of 1:99 is considered. Figure 5 shows the ion densities with an additional neutral X fraction of 1.1% (the properties of X are described below, the fraction 1.1% is set to match input in Heritier et al., 2017). There are only minor differences between results in Figs. 3 and 4. The overall electron density reaches a value of $n_e = 2 \cdot 10^4$ cm^{-3} close to the surface, while Figure 4 shows a smaller value of $n_e = 1.3 \cdot 10^4$ cm^{-3}. In general, the number densities profiles do not differ much in shape, they are slightly shifted to lower densities for the Heritier et al. (2017) settings.

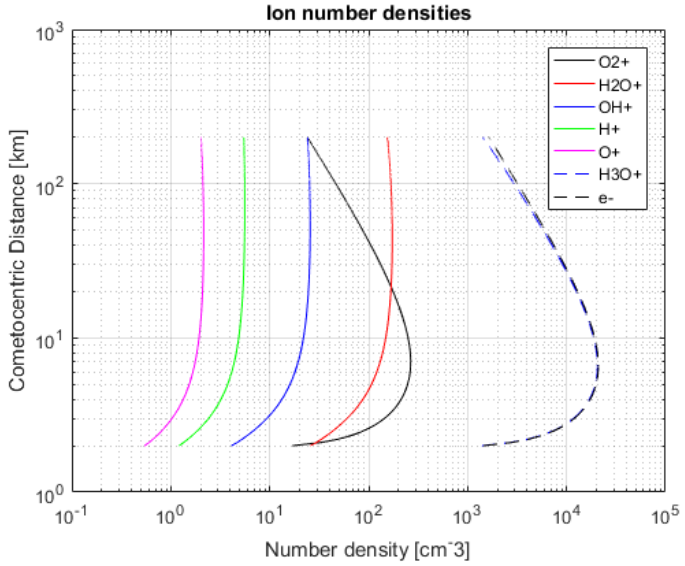

Figure 3: Ion number density profile throughout the cometary coma representing the perihelion conditions of S17.

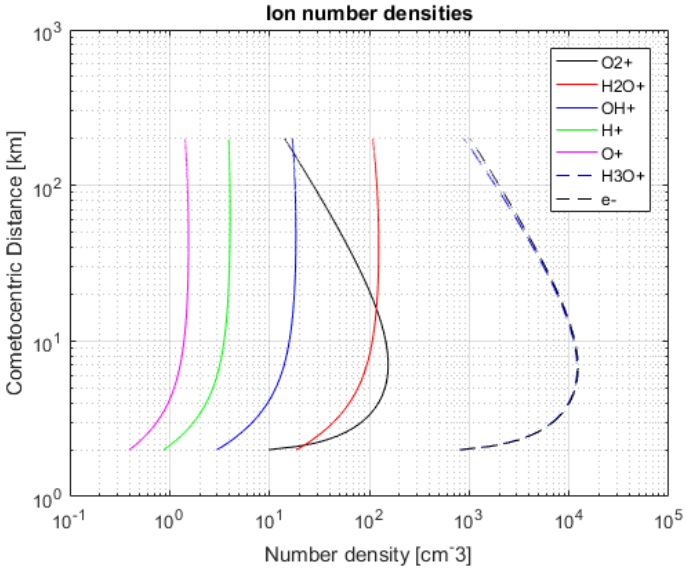

Figure 4: Ion number densities throughout the coma using a scaled down photoionization frequency and a (total) neutral number density that at 180 km is $2 \cdot 10^7$ cm^{-3}, consistent with the input in the simulations presented in Fig. 7 of Heritier et al. (2017).

Comparing Fig. 4 with the results presented in Fig. 7 of Heritier et al. (2017) one notices the discrepancy in the abundance of O_2^+. In Fig. 4 a peak value of $1.5 \cdot 10^2$ cm^{-3} is reached at a cometocentric distance of ~6 km while Heritier et al. (2017) compute a maximum value only of $1.1 \cdot 10^1$ cm^{-3} . There are two reasons for this difference: Firstly, Heritier et al. (2017) did not include O_2^+ production by the photoionization of O_2. This is the major production channel for O_2^+ as shown in S17. Secondly, Heritier et al. (2017) did include species which are reactive with O_2^+ thus enhancing its chemical loss rate and further decreasing the abundance of O_2^+.

Now, Fig. 5 shows an additional simulation, in which we introduce a neutral species called X. The properties of X are similar to NH_3 as discussed in S17; X is not contributing to any production processes of O_2 and H_2O ion species but to loss of O_2^+ (electron transfer) and H_2O^+ and H_3O^+ (proton transfer, forming XH^+). The resulting O_2^+ number density is reduced down to a maximum of $7 \cdot 10^1$ cm^{-3} and XH^+ becomes the dominant species close to the surface with a peak concentration $8 \cdot 10^3$ cm^{-3}. The results of Fig. 5 agree well with the results of Heritier et al. (2017) in many aspects: peak total ion density near 10^4 cm^{-3} at a cometocentric distance of ~4-7 km (broad peak), the switch of the dominance of XH^+ to H_3O^+ near 20 km and similar OH^+ and H_2O^+ profiles in terms of magnitude and shape above ~10 km. Differences in shapes can be seen near the surface which is caused due to the different treatments of expansion velocity (see Section 3.1; in our case, the peaks are somewhat broader). The most notable difference remains, however, the predicted concentration of O_2^+ which in our case is ~7 times higher. As pointed out earlier (and in S17) this difference comes from the fact that we include the direct production of O_2^+ via photoionization of O_2 in our model.

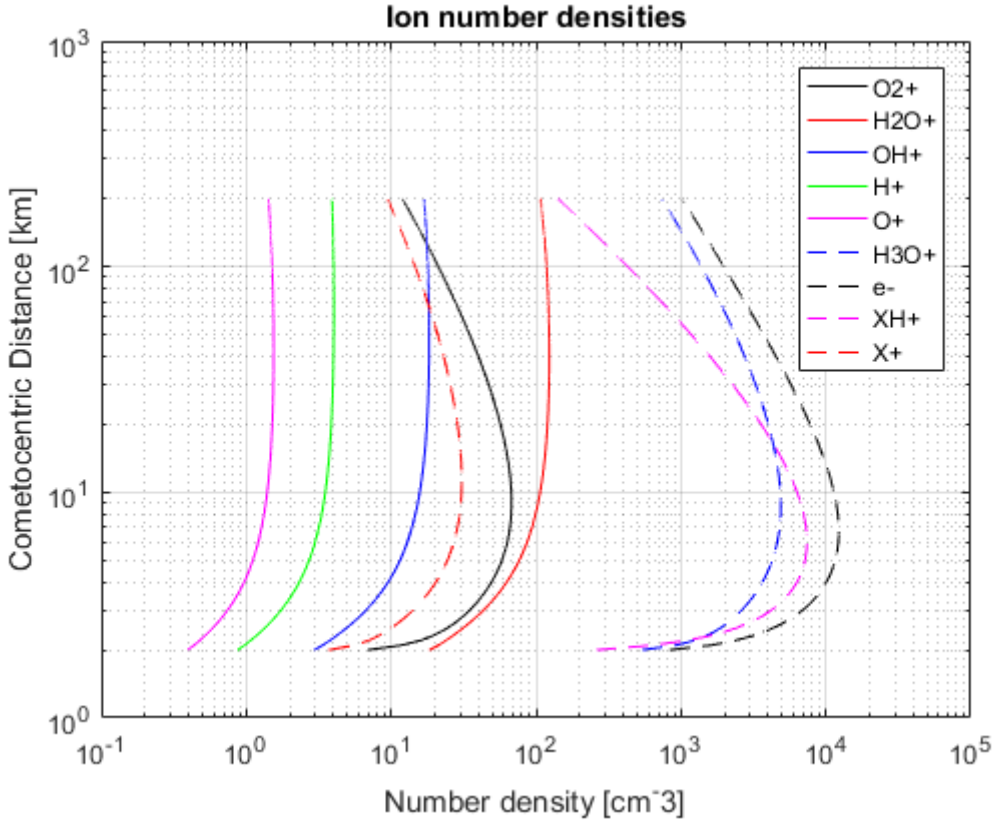

Figure 5: Same as in Fig. 4 but with the introduction of 1.1% of a species X that is reactive with O_2^+.

4. SUMMARY AND CONCLUDING REMARKS

In a previous project work, Scheutwinkel (2017) conducted ionospheric model calculations of the coma of 67P and compared the output with results from Heritier et al. (2017). Discrepancies were seen in the abundances of several types of ions, in particular close to the nucleus (cometocentric distances less than ~10 km). This can be explained by the attenuation effect of the photoionization frequencies, which Heritier et al. (2017) included in their model. Now this effect has been implemented into the model of Scheutwinkel (2017) by numerically solving the Beer-Lambert equation. The resulting attenuated frequencies differed somewhat from the values presented in Heritier et al. (2017) due to differences in the considered solar EUV spectra and the utilized neutral background number densities. For the ion-chemistry model calculations, the input parameters were rescaled to better match those of Heritier et al. (2017). The resulting ion number densities are then in good/reasonable agreement with those of Heritier et al. (2017) with an exception for the predicted abundance of O_2^+ which in our model is ~7 times higher. This is because Heritier et al. (2017) did not include the photoionization production of O_2^+, a process which we have identified as a dominant production channel. As a final remark, it should be noted that neither our model nor the one of Heritier et al. (2017) takes into account the possibility that charged species may be strongly influenced by electric and magnetic fields.

REFERENCES

Bieler, A. et al. 2015, Nature, 526, 678

Gasc, S. et al. 2017, MNRAS, 469, S108

Heritier, K., et al. 2017, MNRAS, in press

Rees, M. H. 1989, Physics and Chemistry of the Upper Atmosphere (Cambridge Atmospheric and Space Science Series; Cambridge: Cambridge Univ. Press)

Rubin, M., et al. 2015. ApJ Lett., 815, L11

Scheutwinkel, K. 2017, Ionospheric modeling of comet 67P/CG with focus on molecular oxygen, 10 credits Project work in Physics & Astronomy, Uppsala University

Schunk, R. W., & Nagy, A. F. 2009, Ionospheres: Physics, Plasma Physics and Chemistry (Cambridge: Cambridge Univ. Press)

Vigren, E., & Galand, M. 2013, ApJ, 772, 33

SOURCE CODE

```
clear all
close all   % clearing plots

% Variables of comet

deltaR=0.1; % units in km
NucleusR=2; %units in km, start of cometary coma
MaxR=200; %units in km, end of cometary coma
DisAU=1.25; %heliocentric distance of comet in AU
Te=300; % temperature of comet in K
```

```
SZangle=89; % solar zenith angle in degrees

SZA=2*pi*SZangle./360; %angle in rad

%initial number density of ions in comet around nucleus [1/cm^3]
%nXX(i,j)  i = time, j = region XX = ion species

nO2P(1,1)=0.01;
nOP(1,1)=0.01;
nHP(1,1)=0.01; % maybe not neccesary because of immediate reaction with H2O
nOHP(1,1)=0.01;
nH2OP(1,1)=0.01;
nH3OP(1,1)=0.01;
nXHP(1,1)=0.01; % ions of molecules XH
nXP(1,1)=0.00; %ions of molecules X
nElec(1,1)=nO2P(1,1)+nOP(1,1)+nHP(1,1)+nOHP(1,1)+nH2OP(1,1)+nH3OP(1,1)+nXHP
(1,1)+nXP(1,1); %sum of all species

%Creating the activity/environment of coma

distanceVec=NucleusR:deltaR:MaxR; %cometocentric vector
Theu=(1e-3)*(-55.5*DisAU+771)*(1+0.171*exp(-(DisAU-1.24)./0.13)); %km/s
expansion velocity
TheQ=(2.58E+28)*DisAU^(-5.1); %Molecules/sec Outgassing rate
deltaT=0.001; %time steps in s

FitHERITIERfactor=(2e+6)/(TheQ/(Theu*4*pi*400*400*1e+15)); %parameter to
fit Heritier et al. (2017) paper
%FitHERITIERfactor=1; %without rescaling, comment out other factor if using

Density=FitHERITIERfactor*TheQ./(4*pi*Theu.*distanceVec.^2*1E+15); %
density profile in 1/cm
TranOut=((distanceVec+deltaR).^3-(distanceVec+deltaR-
Theu.*deltaT).^3)./((distanceVec+deltaR).^3-distanceVec.^3);
%Transportation loss to outer layers of coma

%molecule fractions

fracX=0.00;
fracO2=0.01;
fracH2O=1-fracO2-fracX;


%molecule density fraction

DensityH2O=fracH2O.*Density;
DensityO2=fracO2.*Density;
DensityX=fracX.*Density;

%Density profile of molecules

%figure (1)
%semilogx(DensityH2O,distanceVec,'r')
%hold on
%semilogx(DensityO2,distanceVec,'k')
%semilogx(DensityX,distanceVec,'m--')
%grid on
%xlabel('Number density [cm^-3]')
%ylabel('Cometocentric Distance [km]')
%title('Density profile of neutrals')
```

```
%legend('H2O','O2')
%legend('H2O','O2','X')



% Ionisation frequencies without attenuation
% P is the substitute for +
% first 4 are from H2O
% last 2 from O2

%freqH2OP=5.33E-7./(DisAU.^2); %(1)
%freqOHP=1.49E-7./(DisAU.^2);  %(2)
%freqHP=6.68E-8./(DisAU.^2);   %(3)
%freqOPH2O=8.7E-9./(DisAU.^2); %(4)
%freqO2P=7.56E-7./(DisAU.^2);  %(5)
%freqOPO2=2.35E-7./(DisAU.^2); %(6)
%freqXP=9.3E-7./(DisAU.^2);   % unknown frequency to ionize X to XP


% calculation of the integral expression of Optical depth

deltaZ =deltaR*100000; % dimension is cm, integration variable

%calculation of integrand at different cometocentric distances
for i = 1:1:length(distanceVec)
    for j = i:1:length(distanceVec)
ResultintH2O(i,j) = (TheQ./(4*pi*Theu.*(distanceVec(j)).^2*1E+15)).*(1-
((distanceVec(i))./(distanceVec(j))).^2*sin(SZA).^2).^(-1./2)*deltaZ;
    end
end


A=sum(ResultintH2O,2); %sum over z (integral), vector containing variable
over z0


% Multiplication with cross sections for each H2O ion species

load H2Ophotocross.txt %H2O photocrosssections table

% interpolation of H2Ophotocrosssections in 1 nm bins until 104 nm
for k=1:1:104
    AbsCross(k)=interp1(H2Ophotocross(:,1),H2Ophotocross(:,6),k);
    IoniCrossH2Op(k)=interp1(H2Ophotocross(:,1),H2Ophotocross(:,2),k);
    IoniCrossOHp(k)=interp1(H2Ophotocross(:,1),H2Ophotocross(:,3),k);
    IoniCrossHp(k)=interp1(H2Ophotocross(:,1),H2Ophotocross(:,4),k);
    IoniCrossOp(k)=interp1(H2Ophotocross(:,1),H2Ophotocross(:,5),k);
end
% tau parameter calculation
tauH2OAbs=A*AbsCross;


% intensity with attenuation for every wavelengthbin [1/s cm^-2 nm^-1] on
% every cometocentric distance

load timedfreq.txt %solar EUV spectra table

for i=1:1:length(distanceVec)
for k=1:length(timedfreq)
```

```
intenAtten(i,k)=timedfreq(k).*exp(-tauH2OAbs(i,k).');
end
end


%frequency calculation for H2O with attenuation [1/s]
% deltaLambda = 1 nm, integration variable

freqH2OAbsd=intenAtten*AbsCross.';
freqH2OPd=intenAtten*IoniCrossH2Op.';
freqOHPd=intenAtten*IoniCrossOHp.';
freqHPd=intenAtten*IoniCrossHp.';
freqOPH2Od=intenAtten*IoniCrossOp.';
freqO2Pd=7.56./5.33*freqH2OPd;
freqOPO2d=2.35./5.33*freqH2OPd;
freqXPd=9.3./5.33*freqH2OPd;


%distance correction of frequencies
freqH2OAbs=freqH2OAbsd./(DisAU.^2);
freqH2OP=freqH2OPd./(DisAU.^2);
freqOHP=freqOHPd./(DisAU.^2);
freqHP=freqHPd./(DisAU.^2);
freqOPH2O=freqOPH2Od./(DisAU.^2);
freqO2P=freqO2Pd./(DisAU.^2);  %(5)
freqOPO2=freqOPO2d./(DisAU.^2); %(6)
freqXP=freqXPd./(DisAU.^2);

FitHERITIERfactor2=(3.13e-
7)/(freqH2OP(end)+freqOHP(end)+freqHP(end)+freqOPH2O(end)); %second factor
of Heritier et al. (2017)
%FitHERITIERfactor2=1; %unscaled, comment out other factor above if using
this

freqH2OAbsmatching=FitHERITIERfactor2.*freqH2OAbs;
freqH2OPmatching=FitHERITIERfactor2.*freqH2OP;
freqOHPmatching=FitHERITIERfactor2.*freqOHP;
freqHPmatching=FitHERITIERfactor2.*freqHP;
freqOPH2Omatching=FitHERITIERfactor2.*freqOPH2O;
freqO2Pmatching=FitHERITIERfactor2.*freqO2P;
freqOPO2matching=FitHERITIERfactor2.*freqOPO2;
freqXPmatching=FitHERITIERfactor2.*freqXP;

%attenuated ionization frequencies, not Heritier corrected
figure(3)
hold on
grid on
loglog(freqH2OP,distanceVec,'r')
loglog(freqOHP,distanceVec,'b')
loglog(freqHP,distanceVec,'g')
loglog(freqOPH2O,distanceVec,'m')
loglog(freqO2P,distanceVec,'k')
loglog(freqOPO2,distanceVec,'c')
%loglog(freqXP,distanceVec,'r--')
xlabel('Frequency [1/s]')
ylabel('Cometocentric distance [km]')
title('Ionization frequencies with attenuation effect')
legend('H2O+','OH+','H+','O+H2O','O2+','O+O2')
%legend('H2O+Abs','H2O+','OH+','H+','O+H2O','O2+','O+O2','X+')

%attenuated frequencies, Heritier corrected
```

```
figure(4)
hold on
loglog(freqH2OPmatching,distanceVec,'r')
loglog(freqOHPmatching,distanceVec,'b')
loglog(freqHPmatching,distanceVec,'g')
loglog(freqOPH2Omatching,distanceVec,'m')
loglog(freqO2Pmatching,distanceVec,'k')
loglog(freqOPO2matching,distanceVec,'c')
%loglog(freqXPmatching,distanceVec,'r--')
xlabel('Frequency [1/s]')
grid on
ylabel('Cometocentric distance [km]')
title('#Ionization frequencies with attenuation effect, Hertitier
corrected')
legend('H2O+','OH+','H+','O+H2O','O2+','O+O2')
%legend('H2O+Abs','H2O+','OH+','H+','O+H2O','O2+','O+O2','X+')

%photoionization production
prodH2OP=freqH2OPmatching.*DensityH2O.';
prodOHP=freqOHPmatching.*DensityH2O.';
prodHP=freqHPmatching.*DensityH2O.';
prodO2P=freqO2Pmatching.*DensityO2.';
prodOP=freqOPO2matching.*DensityO2.'+(freqOPH2Omatching.*DensityH2O.');
prodXP=freqXPmatching.*DensityX.'; % production rate Unknown XP
prodION=freqO2Pmatching.*DensityO2.'; %ionization rate of O2
prodElec=prodH2OP.'+prodOHP.'+prodHP.'+prodO2P.'+prodOP.'+prodXP.';
%electron production rate

%Production rates profile of ions

%figure (5)
%semilogx(prodH2OP,distanceVec,'r')
%hold on
%semilogx(prodOHP,distanceVec,'b')
%semilogx(prodHP,distanceVec,'g')
%semilogx(prodO2P,distanceVec,'k')
%semilogx(prodOP,distanceVec,'m')
%semilogx(prodElec,distanceVec,'k--')
%semilogx(prodXP,distanceVec,'m--')
%grid on
%xlabel('Primary production rate [cm^-3 s^-1]')
%ylabel('Cometocentric Distance [km]')
%title('Primary Production Rates')
%legend('H2O+','OH+,','H+','O2+','O+','e-')
%legend('H2O+','OH+,','H+','O2+','O+','e-','X+')


%chemical rate coefficients for ions/molecules, notation APB_CPD means: ion
A+ reacts with neutral B to form ion C+ and neutral D[cm^3/sec]

H2OPH2O_H3OPOH=2.10E-9;
H2OPO2_O2PH2O=4.6e-10;
OHPH2O_H2OPOH=1.59e-9;
OHPO2_O2POH=5.9e-10;
HPH2O_H2OPH=6.9e-9;
HPO2_O2PH=2e-9;
OPH2O_H2OPO=3.2e-9;
OPO2_O2PO=1.9e-11;
OHPH2O_H3OPO=1.3E-9;

% rate coefficents of neutral X with ions
```

```
% coefficients are similar to NH3 to NH4+ production
XH3OP=2.20E-9;
XH2OP=9.45E-10;
XOHP=1.20E-9;
XHP=0;
XOP=0;
XPX=2.2E-9;

%reaction rate of NH3 to NH3+ (O2+ destruction)

XO2P=2E-9;

%reaction rate of NH3+ to NH4+

XPH2O=1.1E-10;


%rate coefficients for recombination [cm^3/sec]
%atomic molecules are not considered because of slow reaction rates

DRH2OP=4.3e-7*(Te/300)^(-0.5);
DROHP=3.76e-8*(Te/300)^(-0.5);
DRO2P=1.95e-7*(Te/300)^(-0.7);
DRH3OP=7.6e-7*(Te/300)^(-0.83);

DRXHP=9e-7*(Te/300)^(-0.6);
DRXP=3.1e-7*(Te/300)^(-0.5);

% total number density in time = i ; region j=1 nXX(i,j) [1/cm^3]
%fist layer above nucleus

deltaT=0.001; %[s]
for i= 2:10000

nO2P(i,1)=nO2P(i-1,1)+prodO2P(1).*deltaT+deltaT.*DensityO2(1).*(nHP(i-
1,1).*HPO2_O2PH+...
    nH2OP(i-1,1).*H2OPO2_O2PH2O+nOP(i-1,1).*OPO2_O2PO+nOHP(i-
1,1).*OHPO2_O2POH)...
    -nElec(i-1,1).*nO2P(i-1,1).*deltaT.*DRO2P-TranOut(1).*nO2P(i-1,1)...
    -nO2P(i-1,1).*DensityX(1).*XO2P.*deltaT; %X destroy O2P
nH2OP(i,1)=nH2OP(i-1,1)+prodH2OP(1).*deltaT+deltaT.*DensityH2O(1).*(nOHP(i-
1,1).*OHPH2O_H2OPOH+...
    nOP(i-1,1).*OPH2O_H2OPO+nHP(i-1,1).*HPH2O_H2OPH)-nElec(i-1,1).*nH2OP(i-
1,1)*deltaT.*DRH2OP...
    -nH2OP(i-
1,1).*deltaT.*(H2OPH2O_H3OPOH.*DensityH2O(1)+H2OPO2_O2PH2O.*DensityO2(1))-
TranOut(1).*nH2OP(i-1,1)...
    -nH2OP(i-1,1).*DensityX(1).*XH2OP.*deltaT; %X destroy H2OP
nOHP(i,1)=nOHP(i-1,1)+prodOHP(1).*deltaT-nElec(i-1,1).*nOHP(i-
1,1).*deltaT.*DROHP-nOHP(i-1,1).*deltaT.*(OHPO2_O2POH.*DensityO2(1)+...
    DensityH2O(1).*(OHPH2O_H2OPOH+OHPH2O_H3OPO))-TranOut(1).*nOHP(i-1,1)...
    -nOHP(i-1,1).*DensityX(1).*XOHP.*deltaT; %X destroy OHP;
nHP(i,1)=nHP(i-1,1)+prodHP(1).*deltaT-nHP(i-
1,1).*deltaT.*(HPH2O_H2OPH.*DensityH2O(1)+HPO2_O2PH.*DensityO2(1))-
TranOut(1).*nHP(i-1,1)...
    -nHP(i-1,1).*DensityX(1).*XHP.*deltaT; %X destroy HP;
nOP(i,1)=nOP(i-1,1)+prodOP(1).*deltaT-nOP(i-
1,1).*deltaT.*(OPH2O_H2OPO.*DensityH2O(1)+OPO2_O2PO.*DensityO2(1))-
TranOut(1).*nOP(i-1,1)...
    -nOP(i-1,1).*DensityX(1).*XOP.*deltaT; %X destroy OP;
```

```
nH3OP(i,1)=nH3OP(i-1,1)+deltaT.*DensityH2O(1).*(nOHP(i-
1,1).*OHPH2O_H3OPO+nH2OP(i-1,1).*H2OPH2O_H3OPOH)-TranOut(1).*nH3OP(i-
1,1)...
    -nElec(i-1,1).*deltaT.*DRH3OP.*nH3OP(i-1,1)...
    -nH3OP(i-1,1).*DensityX(1).*XH3OP.*deltaT; %X destroy H3OP;
nXHP(i,1)=nXHP(i-1,1)+deltaT.*DensityX(1).*(nH3OP(i-1,1).*XH3OP+nOP(i-
1,1).*XOP+nHP(i-1,1).*XHP+...
    nOHP(i-1,1).*XOHP+nH2OP(i-1,1).*XH2OP+nXP(i-
1,1).*XPX)+DensityH2O(1).*nXP(i-1,1).*XPH2O.*deltaT....
-TranOut(1).*nXHP(i-1,1)-nElec(i-1,1).*deltaT.*DRXHP.*nXHP(i-1,1);
nXP(i,1)=nXP(i-1,1)+prodXP(1).*deltaT+(nO2P(i-1,1).*XO2P-nXP(i-
1,1).*XPX)*deltaT.*DensityX(1)...
-DensityH2O(1).*deltaT.*XPH2O.*nXP(i-1,1)...
-TranOut(1).*nXP(i-1,1)-nElec(i-1,1).*deltaT.*DRXP.*nXP(i-1,1);
nElec(i,1)=nO2P(i,1)+nH2OP(i,1)+nOHP(i,1)+nHP(i,1)+nOP(i,1)+nH3OP(i,1)+nXHP
(i,1)+nXP(i,1);

end
nO2P(1,2)=nO2P(end,1); %after loop, the end value sets the beginning value
of the the next region j=2
nH2OP(1,2)=nH2OP(end,1);
nOHP(1,2)=nOHP(end,1);
nHP(1,2)=nHP(end,1);
nOP(1,2)=nOP(end,1);
nH3OP(1,2)=nH3OP(end,1);
nElec(1,2)=nElec(end,1);
nXHP(1,2)=nXHP(end,1);
nXP(1,2)=nXP(end,1);

%layers above first layer

for j= 2:length(distanceVec)-1
for i= 2:10000


nO2P(i,j)=nO2P(i-1,j)+prodO2P(j).*deltaT+deltaT.*DensityO2(j).*(nHP(i-
1,j).*HPO2_O2PH+...
    nH2OP(i-1,j).*H2OPO2_O2PH2O+nOP(i-1,j).*OPO2_O2PO+nOHP(i-
1,j).*OHPO2_O2POH)...
    -nElec(i-1,j).*nO2P(i-1,j).*deltaT.*DRO2P-TranOut(j).*nO2P(i-
1,j)+TranOut(j-1).*nO2P(end,j-1).*...
    (distanceVec(j)^3-distanceVec(j-1)^3)/(distanceVec(j+1)^3-
distanceVec(j)^3)...
   -nO2P(i-1,j).*DensityX(j).*XO2P.*deltaT;
nH2OP(i,j)=nH2OP(i-1,j)+prodH2OP(j).*deltaT+deltaT.*DensityH2O(j).*(nOHP(i-
1,j).*OHPH2O_H2OPOH+...
    nOP(i-1,j).*OPH2O_H2OPO+nHP(i-1,j).*HPH2O_H2OPH)-nElec(i-1,j).*nH2OP(i-
1,j)*deltaT.*DRH2OP...
    -nH2OP(i-
1,j).*deltaT.*(H2OPH2O_H3OPOH.*DensityH2O(j)+H2OPO2_O2PH2O.*DensityO2(j))-
TranOut(j).*nH2OP(i-1,j)+...
    TranOut(j-1).*nH2OP(end,j-1).*(distanceVec(j)^3-distanceVec(j-
1)^3)/(distanceVec(j+1)^3-distanceVec(j)^3)...
    -nH2OP(i-1,j).*DensityX(j).*XH2OP.*deltaT;
nOHP(i,j)=nOHP(i-1,j)+prodOHP(j).*deltaT-nElec(i-1,j).*nOHP(i-
1,j).*deltaT.*DROHP-nOHP(i-1,j).*deltaT.*(OHPO2_O2POH.*DensityO2(j)+...
    DensityH2O(j).*(OHPH2O_H2OPOH+OHPH2O_H3OPO))-TranOut(j).*nOHP(i-
1,j)+...
    TranOut(j-1).*nOHP(end,j-1).*(distanceVec(j)^3-distanceVec(j-
1)^3)/(distanceVec(j+1)^3-distanceVec(j)^3)...
    -nOHP(i-1,j).*DensityX(j).*XOHP.*deltaT;
```

```
nHP(i,j)=nHP(i-1,j)+prodHP(j).*deltaT-nHP(i-
1,j).*deltaT.*(HPH2O_H2OPH.*DensityH2O(j)+HPO2_O2PH.*DensityO2(j))-
TranOut(j).*nHP(i-1,j)+...
    TranOut(j-1).*nHP(end,j-1).*(distanceVec(j)^3-distanceVec(j-
1)^3)/(distanceVec(j+1)^3-distanceVec(j)^3)...
    -nHP(i-1,j).*DensityX(j).*XHP.*deltaT;
nOP(i,j)=nOP(i-1,j)+prodOP(j).*deltaT-nOP(i-
1,j).*deltaT.*(OPH2O_H2OPO.*DensityH2O(j)+OPO2_O2PO.*DensityO2(j))-
TranOut(j).*nOP(i-1,j)+...
    TranOut(j-1).*nOP(end,j-1).*(distanceVec(j)^3-distanceVec(j-
1)^3)/(distanceVec(j+1)^3-distanceVec(j)^3)...
    -nOP(i-1,j).*DensityX(j).*XOP.*deltaT;
nH3OP(i,j)=nH3OP(i-1,j)+deltaT.*DensityH2O(j).*(nOHP(i-
1,j).*OHPH2O_H3OPO+nH2OP(i-1,j).*H2OPH2O_H3OPOH)-TranOut(j).*nH3OP(i-
1,j)...
    -nElec(i-1,j).*deltaT.*DRH3OP.*nH3OP(i-1,j)+TranOut(j-1).*nH3OP(end,j-
1).*(distanceVec(j)^3-distanceVec(j-1)^3)/(distanceVec(j+1)^3-
distanceVec(j)^3)...
    -nH3OP(i-1,j).*DensityX(j).*XH3OP.*deltaT;
nXHP(i,j)=nXHP(i-1,j)+deltaT.*DensityX(j).*(nH3OP(i-1,j).*XH3OP+nOP(i-
1,j).*XOP+nHP(i-1,j).*XHP+...
    nOHP(i-1,j).*XOHP+nH2OP(i-1,j).*XH2OP+nXP(i-
1,j).*XPX)+DensityH2O(j).*deltaT.*nXP(i-1,j).*XPH2O...
    -nElec(i-1,j).*nXHP(i-1,j).*deltaT.*DRXHP-TranOut(j).*nXHP(i-
1,j)+TranOut(j-1).*nXHP(end,j-1).*(distanceVec(j)^3-distanceVec(j-
1)^3)/(distanceVec(j+1)^3-distanceVec(j)^3);
nXP(i,j)=nXP(i-1,j)+prodXP(j).*deltaT+(nO2P(i-1,j).*XO2P-nXP(i-
1,j).*XPX)*DensityX(j).*deltaT...
    -DensityH2O(j).*deltaT.*XPH2O.*nXP(i-1,j)...
    -nElec(i-1,j).*nXP(i-1,j).*deltaT.*DRXP-TranOut(j).*nXP(i-
1,j)+TranOut(j-1).*nXP(end,j-1).*(distanceVec(j)^3-distanceVec(j-
1)^3)/(distanceVec(j+1)^3-distanceVec(j)^3);
nElec(i,j)=nO2P(i,j)+nH2OP(i,j)+nOHP(i,j)+nHP(i,j)+nOP(i,j)+nH3OP(i,j)+nXHP
(i,j);

% (distanceVec(j)^3-distanceVec(j-1)^3)/(distanceVec(j+1)^3-
distanceVec(j)^3)
% is correction term because of different sphere shell sizes with
% increasing radius
end
nO2P(1,j+1)=nO2P(end,j);
nH2OP(1,j+1)=nH2OP(end,j);
nOHP(1,j+1)=nOHP(end,j);
nHP(1,j+1)=nHP(end,j);
nOP(1,j+1)=nOP(end,j);
nH3OP(1,j+1)=nH3OP(end,j);
nXHP(1,j+1)=nXHP(end,j);
nXP(1,j+1)=nXP(end,j);
nElec(1,j+1)=nElec(end,j);
end

for j = 1:length(distanceVec)
    densO2P(j)=nO2P(end,j);
    densH2OP(j)=nH2OP(end,j);
    densOHP(j)=nOHP(end,j);
    densHP(j)=nHP(end,j);
    densOP(j)=nOP(end,j);
    densH3OP(j)=nH3OP(end,j);
    densXHP(j)=nXHP(end,j);
    densXP(j)=nXP(end,j);
    densElec(j)=nElec(end,j);
    CHEM(j)=DensityO2(j).*(densHP(j).*HPO2_O2PH+...
```

```
densH2OP(j).*H2OPO2_O2PH2O+densOP(j).*OPO2_O2PO+densOHP(j).*OHPO2_O2POH);
%chemical production rate of O2+
end


%Number Density profiles of ions


figure (6)
loglog(densO2P,distanceVec,'k')
hold on
semilogx(densH2OP,distanceVec,'r')
semilogx(densOHP,distanceVec,'b')
semilogx(densHP,distanceVec,'g')
semilogx(densOP,distanceVec,'m')
semilogx(densH3OP,distanceVec,'b--')
semilogx(densElec,distanceVec,'k--')
%semilogx(densXHP,distanceVec,'m--')
%semilogx(densXP,distanceVec,'r--')
grid on
xlabel('Number density [cm^-3]')
ylabel('Cometocentric Distance [km]')
title('Ion number densities')
legend('O2+','H2O+','OH+','H+','O+','H3O+','e-')
%legend('O2+','H2O+','OH+','H+','O+','H3O+','e-','XH+','X+')


%production rate compared (Ionization and chemical)

%figure(7)
%semilogx(prodO2P,distanceVec,'k')
%hold on
%semilogx(CHEM,distanceVec,'m')
%grid on
%xlabel('Production rates [cm^-3 s^-1]')
%ylabel('Cometocentric Distance [km]')
%title('Ionization vs. chemical production rate')
%legend('O2+','Chem.')
```